Generation of Complex Waveforms through the Development of a Wideband Digitally Controlled Power Amplifier

Edward Pipe

Slipstream Engineering Design Ltd

epipe@slipstream-design.co.uk

1. Abstract

With ever increasing data rates driving bandwidth and high peak to average power ratio signals demanding higher backoff efficiencies, the typical microwave transmitter is limited by a bandwidth/ efficiency trade-off made in the output stage RFPA. Recently LMBA developments have suggested there is a route to bypass the fundamental bandwidth limitation of typical high-backoff topologies, while still achieving enhanced backoff efficiency over large bandwidths.

More generally, this promise extends to remove the limitations of typical RF transmitters, and drive toward frequency and output power agnostic hardware, where digital control of the RF signal can be utilised to optimise the output impedance of the RFPA in real-time. This presentation will discuss some of the investigations and experiments undertaken to gain a better understanding of the challenges and limitations of the LMBA approach, and to explore the potential for digitally controlled RFPAs for Software Defined Radios (SDR) of the future.

2. Challenge of Efficient, Wide Bandwidth Transmitters

Two main challenges are being addressed with transmission of a modern telecommunication signal:

- Peak to average ratio (PAR)
    - Instantaneous bandwidth and recovery time.
    - Efficiency
- RF Bandwidth
    - Accessible radio spectrum.

The advent of affordable, direct conversion software defined radios has reduced the bespoke analogue component count in many RF transceivers (especially in the sub mmWave bands). This has in turn created opportunities for greater hardware flexibility, indeed when receiving it is now possible to simply alter register values and the frequency of operation can change. When transmitting however, the hardware is still limited to specific frequency bands, especially in cases where the RF power levels have severe consequences for dissipation, and handling.

Modern direct conversion SDRs are increasingly able to linearly reproduce signals over a very large bandwidth, held back only by the optical links and digital hardware providing the data. This allows analogue realisation of very broad bandwidth, complex signals. Users wish to transmit these signals accurately at high power levels and so the RFPA designer must answer the increasing linearity requirements of the bandwidths, whilst achieving sufficient efficiency that the RFPA doesn't fail from overheating and can operate within the limits of the available power supply.

While ever-larger data rates and bandwidths add difficulty to the RFPAs task, they also create opportunity. When synchronised these SDRs can drive RFPAs simultaneously and coherently, allowing for adjustment of the schemes employed to retain amplifier efficiency.

3. Wideband or Efficient?

Traditionally the heading above represents the available options. Wide bandwidth and high efficiency do not coexist. Load Modulated Balanced Amplifier (LMBA) technology is allowing a blurring of the lines and presents an exciting opportunity for future RF Transmitters.

3.1. RF Transistor Output Matching

At the simplest level, LMBA offers a methodology through which the output impedance presented to an RF FET can be modulated. To explain this the following section outlines some fundamental theory on which the thinking depends. This begins at impedance matching the output of the RF power device.

Before considering parasitic components, an RF FET operates much the same as any other FET. As shown by Figure 1; In small signal operation the current through the drain-source (i_{ds}), is directly proportional to the voltage across the gate source terminal (v_{gs}).

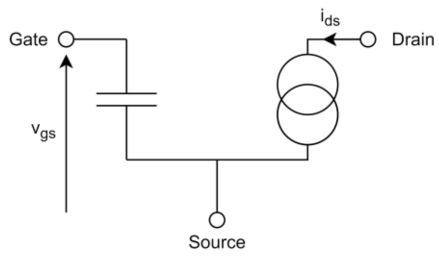

Figure 1: FET Model with no output parasitic components.

The fundamental output impedance of the transistor is calculated from the inverse of the gradient of the line drawn in Figure 2. This provides a real impedance to which the proceeding network must be matched for high efficiency and output power.

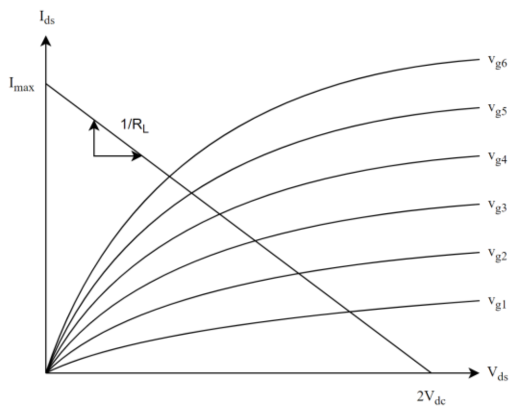

Figure 2: Example Load Line Graph for a FET. The FET exhibits a different Drain Current vs Drain Voltage response depending on gate voltage. When designing an RFPA the ideal load impedance to present to the intrinsic junction of the device is calculated from the inverse of the gradient of a line between the maximum current and 2x the Drain Voltage.

The challenge arises when the designer tries to match to this impedance. Since the intrinsic semiconductor junction cannot be accessed directly, intrinsic passive components represent the unavoidable physical effects of the transistor construction and its package. An example of a HEMT model is shown in Figure 3. This contains reactive elements which adds electrical length, or frequency dependant phase rotation between the drain-source channel of the transistor and the output bond wires or package pin. This increases complexity, since this reactance must be cancelled in the matching process.

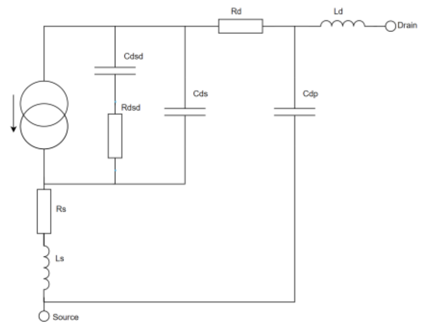

Figure 3: Output side of HEMT transistor model including passive parasitic components. [1]

When operating at a single frequency, this can be a simple complimentary match, so the optimum 'real' load impedance is presented, and maximum power or efficiency operation is achieved.

When viewed over a bandwidth, this reactance rotates clockwise on the smith chart. To achieve performance across the operating frequency band, the designer must present the compliment of this impedance at every frequency. Any passive network that can be manufactured will always have electrical length. The complimentary impedance profile has a negative electrical length. Creation of the proper complimentary impedance isn't possible with a passive circuit. The designer is left to create hoops and loops that match the ideal response as closely as possible. The blue trace in Figure 4 shows an example of what an unmatched transistor S22 looks like on a smith chart.

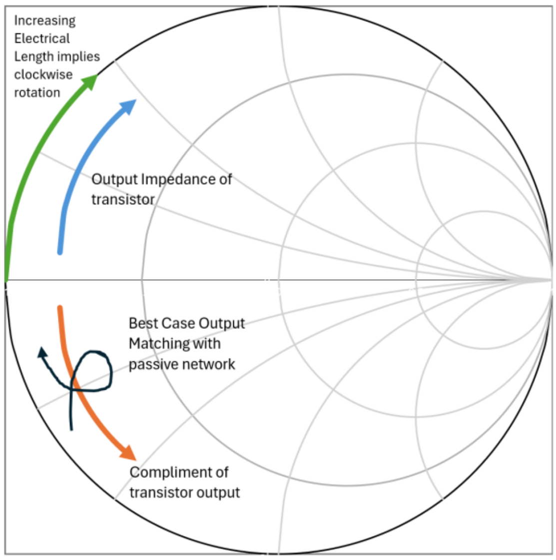

Figure 4: Transistor Output Impedance has increasing electrical length over frequency. True complimentary matching requires a negative phase rotation in the matching network across frequency. Best Case for passive matching is to create a loop in the phase rotation.

3.2. Bode-Fano Criterion [1]

This passive matching limitation is described more generally by the Bode-Fano criterion, a theoretical limit on the maximum reflection coefficient that can obtained with an arbitrary passive matching network.

This means that through passive matching networks, no matter how lossless, or cleverly designed, it will never be possible to achieve a perfect wideband response that correlates directly with the driving circuit. For an amplifiers output, it isn't possible to perform perfect matching for power and efficiency over a bandwidth with a passive circuit.

3.3. Load Modulation [2]

Load Modulation enables the designer to present a range of load impedances to the output of the RFPA. This allows the device to be electronically tuned, usually for efficiency, over a range of output powers -as per the Doherty case. Figure 5 shows the simplest case for load modulation, where two current sources inject current into a common load. When $i_2 = 0$, the impedance Z_1 is equal to Z_L. If a current is injected into Z_L from i_2 Then Z_1 is described by Equation 1. This means that by altering the phase and amplitude of i_2, the complex load impedance, seen as Z_1, is also altered.

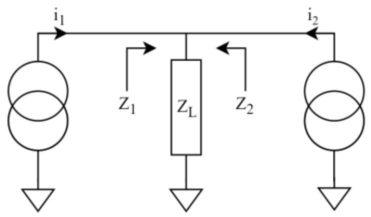

Figure 5: Simplest case for load modulation.

$$Z_1 = \left(1 + \frac{i_2}{i_1}\right) Z_L$$

Equation 1

Doherty's take advantage of this technique to alter the impedance seen by the carrier amplifier depending on the power level present. The fundamental load impedance is modulated from 100Ω at 6dB output power backoff, to 50Ω at peak output power. The net effect is to increase the efficiency of the overall PA over its power backoff range by optimising the voltage swing across the drain-source terminal of the RF device. This topology is well documented and so won't be covered here. However, it relies upon a passive ¼ wavelength impedance inversion structure to perform a 90-degree phase rotation. This only operates at a fixed frequency, Performance falls away as the bandwidth is increased. This leads to inherently narrowband operation, limiting the useful bandwidth of the amplifier.

4. Load Modulated Balanced Amplifier [3]

The basic LMBA, shown in Figure 6, suggests a way to address the fundamental bandwidth limitation in the Doherty configuration while retaining the efficiency performance improvements. The configuration uses two RFPAs, balanced between two quadrature hybrid couplers. The isolated port of the hybrid coupler provides an input for RF power to be injected into the RFPA output. This input is naturally isolated from the bulk of the RF power being generated by the BPA and so provides a suitable place for power injection. A convenient way to think about the occurrence of load modulation here is to consider that when RF power is injected backwards toward the BPA output, a standing wave ratio occurs between the forward and reverse going waves. From the perspective of the BPA devices this produces a modulated load impedance. The advantage of this approach, over that of a Doherty for example, is that both the power level and phase of this returning wave can be designed for over a bandwidth, so a complex and arbitrary reflection coefficient can be realised. The reverse going wave is also reflected off the current source at the BPA output and recombines in the load. This means that any RF power used to control the BPA impedance is recovered in the load and so doesn't retract from the overall system efficiency.

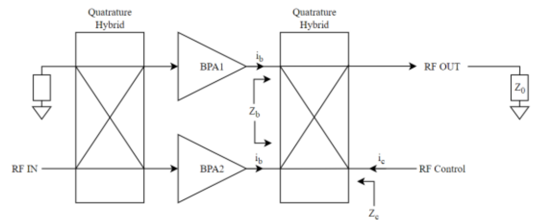

Figure 6: Basic LMBA. Two amplifiers balanced between two 90° hybrid couplers. A control signal, at the same frequency as the RF signal, is injected into the isolated port of the hybrid couplers to modify the impedance seen by the Balanced Power Amplifiers (BPAs).

Following analysis of the 4-port Z parameters of the quadrature hybrid, one arrives at Equation 2. The impedance seen at the BPA output is described as a function of the system characteristic impedance, of the ratio of the magnitude of individual BPA and control currents, and their phase difference.

$$Z_b = Z_0 \left(1 + \sqrt{2}\frac{i_c e^{j\theta}}{i_b}\right)$$

Equation 2

Continuing the analysis, equations can be derived to generate modulation contours for the impedance Z_b according to the relative currents. These allow the load impedance being seen by each BPA to be quantified in terms of reflection coefficient, ρ_b, and utilised as part of the design process. Equation 3 shows the relationship between the magnitude of the reflection coefficients and α, which is defined here as the ratio of the RF control signal power to the RF power being transmitted by a single balanced amplifier. I.e. reverse over forward going waves. The angular component of the synthesised reflection coefficient is equal to the phase difference between the balanced and control RF signals.

$$|\rho_b|^2 = \frac{\alpha}{(2+\alpha)}$$

Equation 3

Where:

$$\alpha = \frac{P_{control}}{P_{balanced}}$$

Equation 4

Figure 7 has been created to assist with visualisation of the required alpha ratio to achieve fixed impedance values along the real axis from 0 to 50Ω, in a 50Ω system. This is a special case where the balanced current and control currents are in phase. The example shows that for a 10dB α ratio, ~32R is achieved.

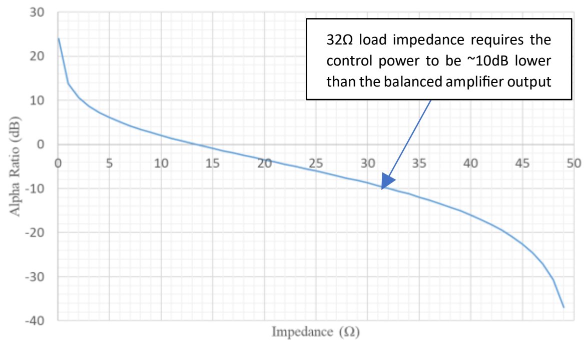

Figure 7: α ratio required to achieve a Real Impedance in a 50Ω system with no phase shift between balanced and control RF signals in an ideal LMBA.

As discussed earlier, the phase between the balanced and control currents adjusts the phase of the complex impedance. This can be visualised on the smith chart as shown in Figure 8. The ratio of the power levels sets the magnitude, whilst the phase angle between the two signals sets the angle of the reflection coefficient.

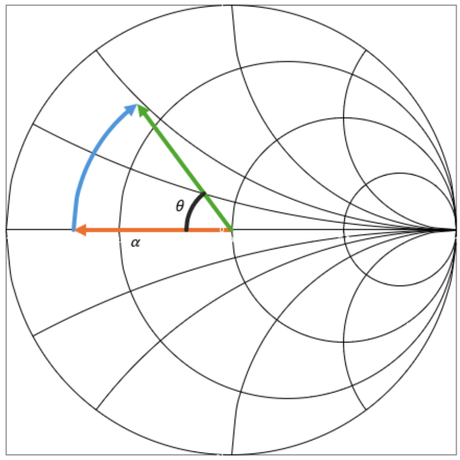

Figure 8: The ratio of control power to balanced power, α, sets the magnitude of the reflection coefficient. The phase between the two RF signals sets the angle, θ .

This tells us that if the designer selects the power and phase of the control power relative to the main balanced amplifier power then, much like a load pull tuner, they can electronically modulate the load impedance seen by the balanced amplifiers to enhance performance.

5. Pseudo-Doherty LMBA [4]

To emulate the backoff efficiency performance of a Doherty without the bandwidth constraint, the Pseudo-Doherty LMBA (PD-LMBA) was devised. This topology utilises a wideband Class-AB Control Power Amplifier (CPA) as the carrier amplifier, whilst the BPA amplifiers are biased deep into class-C, so act only at large input signal levels. It takes advantage of the control power recovery to maximise system efficiency performance.

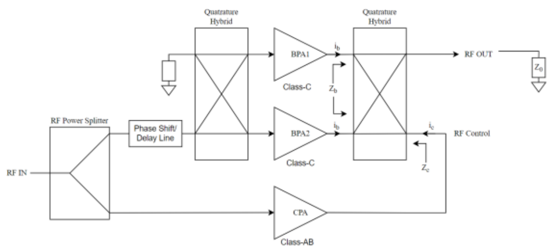

Figure 9: Single PD-LMBA. For PD-LMBA operation, the CPA is biasing in Class-AB, whilst the BPAs are biased into Class-C. The Phase Shifter provides the optimum control signal phase to the BPAs.

The CPA is designed to saturate at the point at which peak backoff efficiency is desired. After this the BPAs begin to turn on. The BPAs are pre-matched for best efficiency at saturation in 50Ω. Careful consideration is given so that up until the power output at the intended backoff level, P_{OBO}, their impedance follows the trajectory for maximum efficiency as per the standard Doherty case.

There are two regions of operation for a PD-LMBA (indicated in Figure 10):

1. **Low Power Region**; Defined by $P_{RF\ OUT} < P_{OBO}$. Where $P_{RF\ OUT}$ is the total RF output power, and P_{OBO}. In this region only the CPA is operational. It is designed to reach saturation and maximum efficiency at P_{OBO}. In this region the impedance seen by the CPA, $Z_{c,LP}$, is the characteristic impedance since all power is reflected off the BPA output into the Load at the output of the hybrid. The BPA output impedance, $Z_{b,LP}$, is infinite since it consists of a current source with no input drive at low power, Equation 5:

$$Z_{c,LP} = Z_0$$

$$Z_{b,LP} = \infty$$

Equation 5

2. **High power region**; Where $P_{RF\ OUT} > P_{OBO}$ and $P_{RF\ OUT} < P_{MAX}$ (the maximum saturated output power). In this region the BPA turns on increasingly with output power. The BPA is pre-matched to 50Ω at saturation. At P_{OBO}, the maximum load modulation occurs. This is the point where α is largest. In this region the impedance seen by the CPA is maintained since the current source at the BPA output still reflects any incident RF power. As the input drive in the high-power region is sufficient to turn the transistor on, the output impedance of the BPA matches Equation 2 above.

Figure 10 has been created to help illustrate the contributions to output power from the BPA and CPA. Efficiency is maintained in the region between P_{OBO} and P_{MAX} by carefully aligning the phase difference of the input and output of the control amplifier, while setting up the biasing so that as the output power increases, the BPA requires less load modulation to achieve higher efficiency performance.

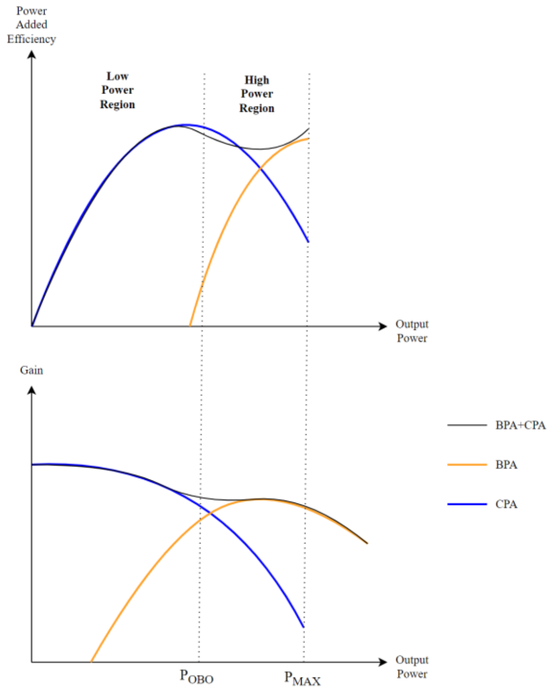

Figure 10: Illustration of the efficiency and gain contribution from CPA and BPA in PD-LMBA configuration. Before P_{OBO}, the CPA contributes the main output power to the load. Afterward, the BPA turns on and transitions to take over the main output power at P_{MAX}. The CPA remains saturated over the high-power region.

6. LMBA Practical Validation

An initial practical investigation was undertaken to validate the theory described in sections 4 and 5. To achieve load modulation for a range of complex impedances the main and control RF inputs were driven separately to control α and θ. It was undertaken to drive these using a bespoke modern multi-channel digital front end contained inside a high-performance SDR. This was then used in the test and development of initial breadboard and prototype amplifiers.

6.1. RFSoC Based Digital Test Platform

A key requirement to develop and validate LMBA technology is to be able to drive the BPA and CPA inputs separately. To realise this dual input approach, a test platform capable of driving two phase coherent and time synchronised RF channels, where phase and amplitude can be controlled digitally, is required. A bespoke control algorithm for this application was designed using the Simulink model-based design process and ported onto the AMD Gen3 RFSoC platform. The algorithm enabled the frequency-dependant control of the complex baseband signal on a sample-by-sample basis. Digital techniques were used to perform stepped attenuation, and phase shifting depending on the frequency of operation. Figure 11 illustrates the model-based design approach, the algorithm developed in Simulink then ported down onto the hardware in stages.

Figure 11: Test Platform developed using model-based design from the Simulink RFSoC toolchain, down compiled into HDL, and run directly in the FPGA fabric.

Figure 12 shows the platform block diagram. A hardware agnostic HDL block sits on the FPGA contained in the Gen 3 RFSoC. This provides the functionality to divide the input IQ baseband data into main and control channels and perform signal processing to drive a dual input amplifier. There are 3 essential features: amplitude scaling, phase adjustment and fractional delay filtering. The amplitude and phase adjustment allow setting of the LMBA α ratio and coarse CPA phase. The fractional delay filter enables the user to create a time delay that corresponds with a small RF phase shift, allowing a frequency-dependent phase to be implemented. This enables the optimum control phase to be presented on a sample-by-sample basis. MTS API, shown as part of the system, is the synchronisation function built into the RFSoC platform to allow time synchronisation of the RF data converters and enable coherent outputs with a constant phase offset.

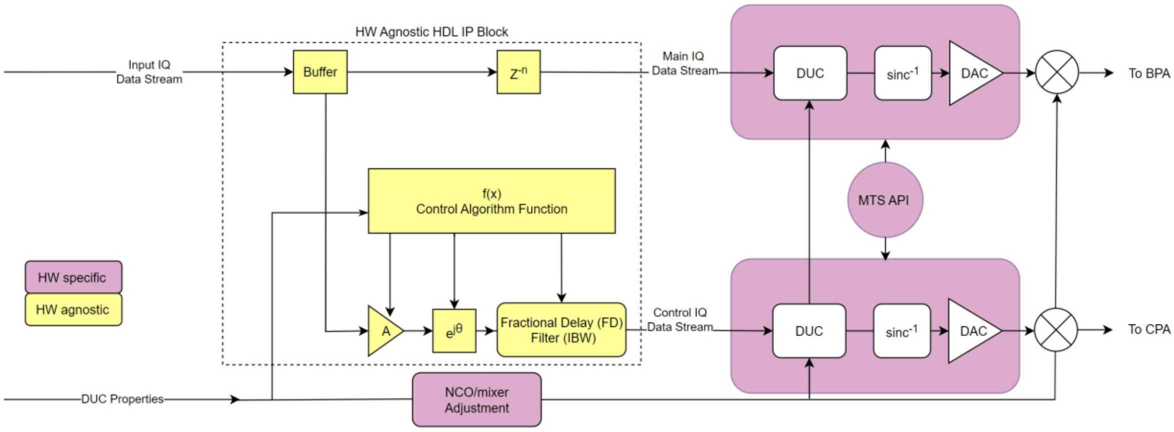

Figure 12: LMBA Test Platform block diagram.

A GUI (Figure 13) was developed to interface directly with the test platform on the FPGA during operation. Control of the platform is facilitated by three tabs:

- Control – Allowing the user to configure the output waveform in carrier frequency, modulation, pulse, amplitude, phase and time delay.
- Config. – Allowing the user to reset the application and reconfigure settings required for communication with the platform.
- MATLAB – Providing input and output terminals to the MATLAB workspace instance which govern the platform.

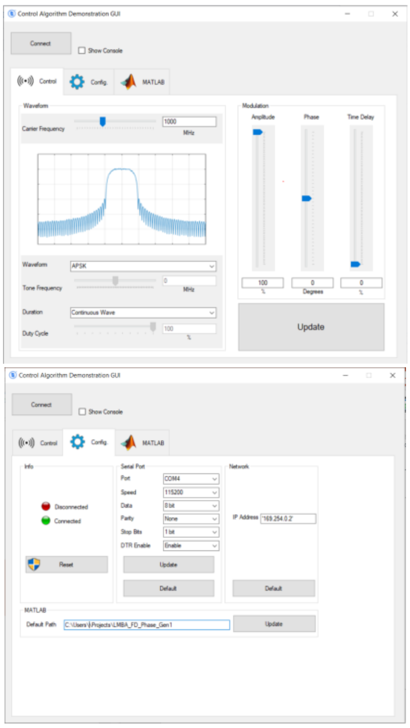

Figure 13: Test Platform GUI.

The intended phase performance of the Test Platform is shown in Figure 14. The coarse phase is selected with the phase shift calculation. A time delay is then applied to achieve a phase slope over the instantaneous bandwidth of the baseband data.

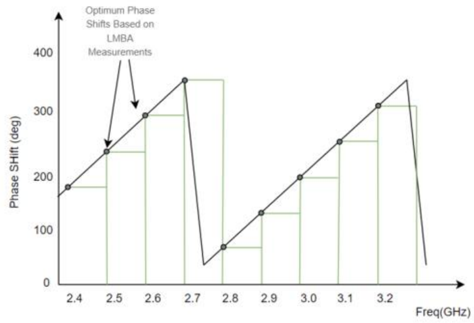

Figure 14: Intended phase difference of test platform between BPA and CPA inputs.

Figure 15 shows the measured performance of the test platform over 2.4-3GHz using 100MHz coarse frequency steps with phase slope provided by the fractional delay filter. Slight performance degradation at the band edge can be seen due to the fractional delay reaching the limits of its operation. The worst-case example of this is at 2.9GHz, where the phase error was measured at -8°.

a)

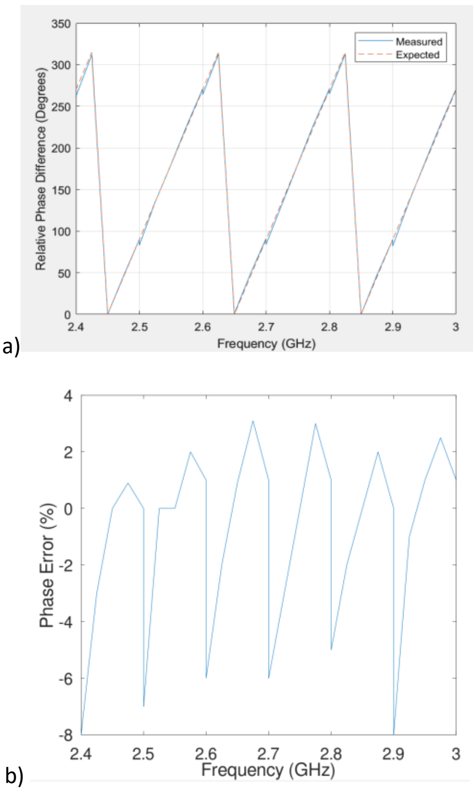

b)

Figure 15: Measured vs expected performance of the phase response of the test platform from 2.4-3GHz. Fractional delay performance begins to drop at the outer edges of the 100 MHz frequency band (a). Phase error from Figure 15(a) plotted over frequency (b).

6.2. Electronic Vs Mechanical Load Pull

To prove that the theoretical load modulation functionality can work. An initial breadboard PA was designed and manufactured. This featured SMT discrete transistors (QPD0020) and off the shelf quadrature hybrid couplers (IPP-7015). The design spanned 2.4-4.2GHz and was hand-built on a simple 2-layer Rogers 4350 PCB fixed to an extruded aluminium heatsink.

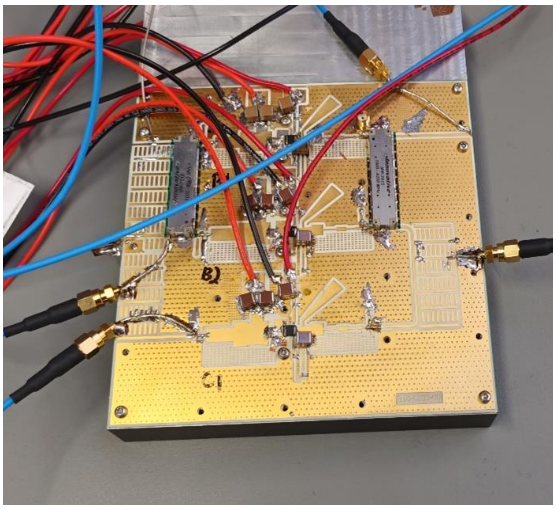

Figure 16: Initial LMBA Prototype.

As can be seen from Figure 16, it was an initial breadboard. This allowed us to move forward and undertake an initial set of measurements and better understand LMBA operation. In collaboration with the Compound Semiconductor Applications Catapult a mechanical load-pull of a single BPA was captured. This test was then repeated at Slipstream Engineering Designs facility, using the LMBA. The results, displayed in Figure 17 (a) and (b), show excellent agreement in both performance and contour shape, verifying the theory presented by academia. The electronic load pull provided slightly lower efficiency and a slightly different contour shape since the LMBA test setup also included the non-ideal performance of the hybrid coupler and the PCB.

At this point we were confident that we could implement and utilise the LMBA technique.

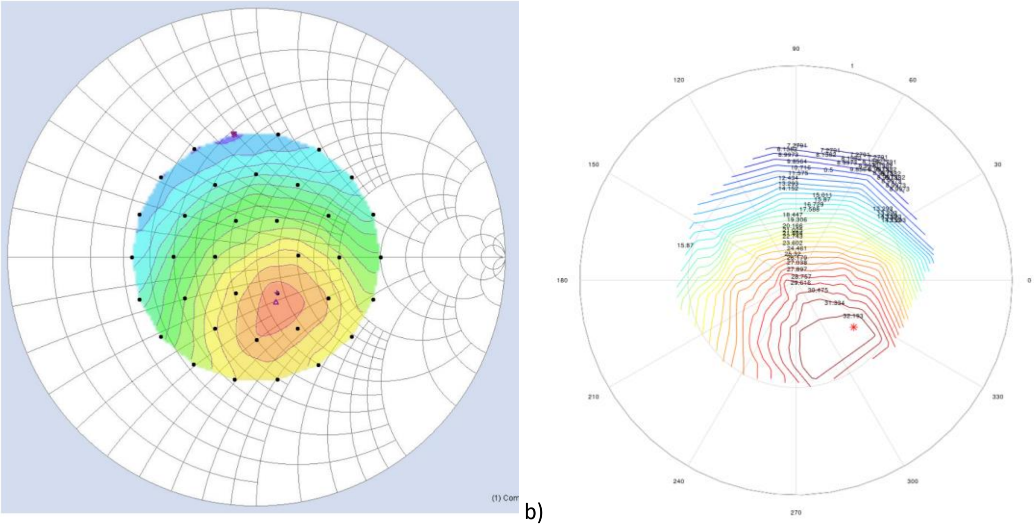

Figure 17: Mechanical (a) vs Electronic (b) load pull contour comparison.

7. Prototype PD-LMBA

Using learning from the initial breadboard lab testing, a robust and higher performing amplifier test platform was developed. In this case, we designed 3 wideband Class-AB PAs using unmatched transistors from Macom (Wolfspeed). We configured these to test and characterise several LMBA configurations with a focus on developing experience and understanding rather than performance for a specific application. A drain switching circuit was included on each amplifier design for easy on/off control of each amplifier, depending on the testing being performed. Flange and pill packages were used, and the PCB was laminated to an aluminium thermal baseplate with conductive adhesive. This allowed much greater thermal resilience than our breadboard design. If during load modulation development an amplifier went inefficient, or unstable, it would have a greater chance of survival. This robust development platform provided us with an opportunity to implement alternate matching network techniques, to search for and find optimum matching topologies to help meet bandwidth performance and minimise PCB area.

As before, these amplifiers were designed to operate over 2.4-4.2GHz, focussed on maximum drain efficiency and gain of the overall amplifier. For integration into a PD-LMBA, where the phases of BPA and CPA need to be closely aligned, it's important to keep the matching network electrically short to minimise any phase adjustment line length needed to achieve the optimum broadband phase shift.

These were all contained on a single amplifier PCB and cascaded in a drive chain to allow characterisation and operation without off the shelf test power amplifiers. Figure 18 shows the built-up Prototype LMBA. The LMBA configuration can be seen on the right-hand side. In the top left, output matching networks can be seen for measurement and evaluation, alongside the printed directional coupler.

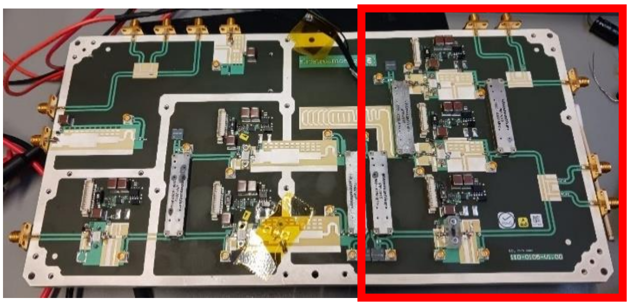

Figure 18: Full Protype LMBA hardware PCB Assembly, mid-development. LMBA configuration can be seen in the red box.

7.1. Phase Characterisation

It's critical to ensure that the PD-LMBA is efficient over the whole backoff range, not just at the power backoff and saturated points. Using our digital test platform to drive the CPA and BPA inputs from separate DACs, we were able to characterise different scenarios to further prove the reported literature. To characterise the performance at different phase differences, the CPA and BPA inputs were initially driven separately using the test platform developed in section 6.1.

Measurements such as Figure 19, show the effect of both control phase and α ratio on the efficiency. Peak efficiency is obtained from the optimisation of both.

Figure 19: Control phase swept for 3 different alpha ratios at a fixed BPA input power.

Figure 20 shows the effect of varying the phase of the control signal relative to the main signal. For this, the BPA was biased into Class-AB and the alpha ratio was maintained at 0.3. 5 phase states were stepped through in 72° steps to achieve 360° phase rotation. The CPA power contribution is measured using the printed directional coupler and then subtracted from the measurement results. By keeping a constant alpha ratio, the effect of the BPA-CPA phase difference on BPA performance is isolated. The maximum efficiency is obtained at almost the same phase across the range of output power, changing a small amount as the amplifier compresses and the peak efficiency impedance changes.

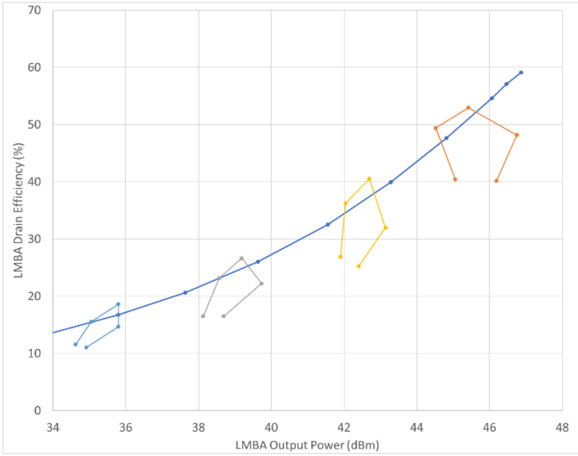

Figure 20: 2.5GHz Balanced power sweep (blue), overlaid with the efficiency results when an α ratio of 0.3 is introduced and the phase of the control signal is rotated. The efficiency is modulated over the 5 different phase states tested. The phase shift to achieve the maximum efficiency is the same at every power level.

To operate across the full frequency range of the amplifier, the optimum phase-frequency relationship must be characterised. So, we biased the amplifier to operate in a PD-mode (Class-C BPA, Class-AB CPA) and drove the BPA input to output 6W. We then added a control signal to achieve an alpha ratio of 0.3 and performed a fine phase sweep at each frequency. By performing a best fit measurement, we characterised the optimum phase-frequency relationship. Since this is roughly linear and negative in slope, it can be approximated by implementing a delay line between the input power splitter and BPA input to create a negative phase rotation with frequency. Some coarse phase measurement results are shown in Figure 21.

Figure 22 shows the output of the phase-frequency characterisation. It plots the phases at which peak efficiency is observed across the bandwidth of the amplifier. This was then modelled using a linear approximation and implemented using sections of transmission line available on the PCB. The optimum phase shift was then retested and can be seen in the yellow trace.

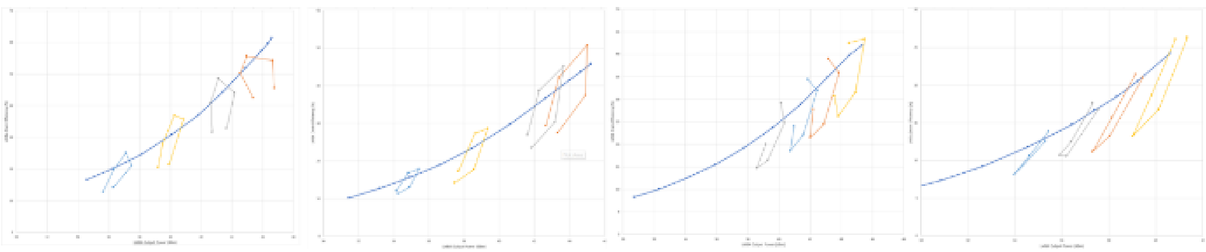

2.5GHz 3GHz 3.5GHz 4GHz

Figure 21: phase rotations performed across frequency. Some initial, coarse, results shown here. Finer sweeps were then taken around each maximum point to find the phase-frequency relationship for maximum efficiency.

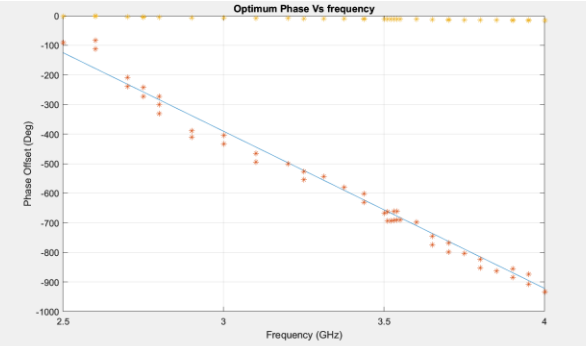

Figure 22: The orange line shows measurements of the optimum phase shift for peak efficiency across frequency. The blue line shows the linear approximation of the peak efficiency point measurements. The points are the initial measurement repeated once the phase shifter had been implemented.

7.2. Practical Learnings

At turn on, a low frequency oscillation in the 170 MHz region occurred at low drain voltages. A resistive element was initially added in series with the input of the amplifier, this allowed the amplifier to be turned on in a stable and controlled way but compromised overall gain performance. Removing this and replacing the gate feed inductor with a 500R resistor achieved the gain profile shown in the red trace below. Measured and simulated gain plots are shown in Figure 23.

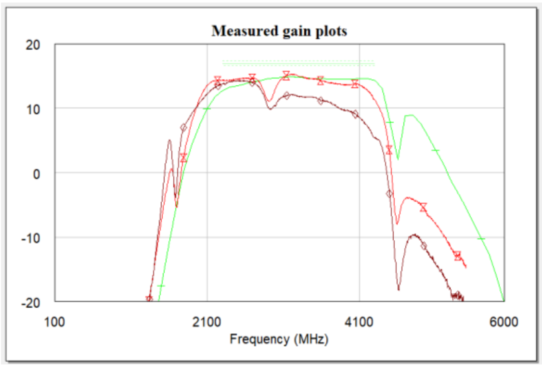

Figure 23: Green: Simulated Gain plot for the BPA when biased in Class-AB. Brown: measured gain plot when stabilised with 100Ω resistor in series with input matching network. Red: Measured gain when stabilised with 500Ω resistor in place of gate bias inductor. The notch at 2.9GHz was due to an unexpected resonance in a tuning capacitor when compared to provided manufacturer data.

During initial testing, a resonance was also present in-band, see Figure 23. This was investigated and isolated to a capacitor that was a key part of the output matching network, positioned close to the device. This resonance wasn't present in the S-parameter data for this specific capacitor and a replacement capacitance solution had to be found and implemented on the hardware. We were unable to find a capacitance solution which provided the performance promised by the original data, and so the final performance of the BPA stage was limited.

There was an issue with the footprint of the off-the-shelf hybrid coupler and return loss of the high-power termination at the input hybrid isolated port. This added ripple to the hybrid performance which affected the balance of the two amplifiers.

7.3. Single Input PD-LMBA Results

Once the optimum phase was characterised, an initial bias was set on each device and another hybrid was placed at the input to allow single input drive to collect some characterisation results. The P1dB Drain Efficiency results are shown in Figure 24. Results were only captured up to P1dB point, to limit CPA gate current.

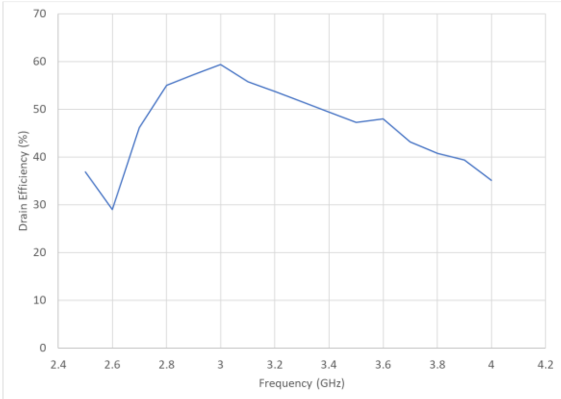

Figure 24: P1dB Drain Efficiency results of the PD-LMBA with single input drive (utilising an analogue phase shifter). Device bias voltage was set up and held constant for every measurement point.

A power sweep for 3.6GHz in this configuration is shown in Figure 25. When in PD-LMBA configuration, the amplifier achieves an efficiency improvement when compared with the balanced Class-AB case. The classic 'Doherty' efficiency curve begins to become evident.

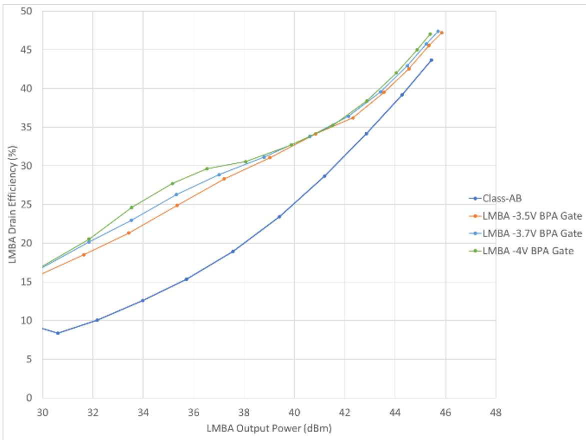

Figure 25: Drain Efficiency Improvement in PD-LMBA configuration at 2 different BPA bias depths vs the balanced case at 3.6GHz.

This improvement wasn't reflected in the PAE since the gain of this single input configuration was very low. Improving this is part of the next steps for our research and illustrates a limiting challenge to the single-input PD-LMBA topology.

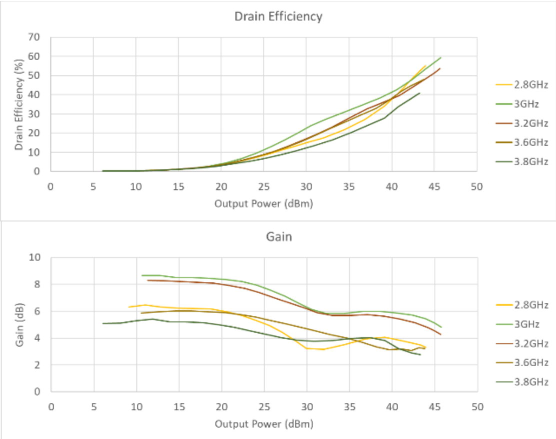

Figure 26: Example measurements of swept Gain and Efficiency vs Output Power for single input case.

Figure 26 shows some example plots of gain and drain efficiency. Gain droop in the centre of the plots can be seen. This is the region where the BPA begins to take over the CPA.

7.4. Discussion

As part of this project many challenges were identifies and overcome. The following points haven't yet been fully addressed in this work and others, so have been discussed in some detail below:

Balancing: In the true Doherty configuration, adjustment of the Class-C bias only involves 1 amplifier and so only 1 parameter that can be adjusted. In the PD-LMBA case the biasing is more nuanced since there are two parameters to adjust simultaneously. To measure balance when performing biasing in Class-C, the amplifier must be driven to self-bias with input power and then have its applied d.c. bias adjusted until the power levels match. Bias difference manifests as imbalance which wastes output power.

Adaptive biasing: Over frequency the necessary gate bias points change for each amplifier. The bias must be adjusted to bring the gain of each amplifier into line to achieve the best overall PAE. This is referenced in [4] where optimum performance is presented with an independent bias point for each frequency measurement.

Linearity & recovery time: In the single ended PD-LMBA topology, the CPA continues to be driven, even when the input signal is sufficient to drive the BPA well into saturation. This overdrives the gate of the CPA, reducing reliability and increasing the recovery time of the CPA. This means that for a single input PD-LMBA being driven with a high PAPR signal, the linearizable modulation rate is always going to be limited by the 'memory effects' caused by this overdrive on the CPA.

Gain: 3dB of input drive power is always wasted in the input RF power split. At low power the BPAs aren't active, and at high power, the CPAs are saturated and contributing a minute amount to the overall output power. Due to Bode-Fano, it is difficult to achieve a well-matched input to the RF devices over such a broad bandwidth. As there is gain over such a broad bandwidth, it is also more difficult to achieve stability. Reduction in S_{12} feedback is performed by adding lossy components into the bias lines and or input of the wideband design. Tuning a resonance isn't easy since it will likely be tuned to a different part of the amplifier's frequency band. Combining all these factors together means that the overall PAE of single input PD-LMBA designs are likely always fundamentally limited by the stable gain that the designer can achieve.

8. Next Steps

Following the discussion in section 7.4 potential advantages can be seen to lie in the utilisation of the digital control functionality made available by modern SDR platforms. Several experiments are to be constructed to help inform this understanding and investigate whether the trade-off in complexity is worth it for the potential performance improvements.

The experiments below have been conceived to further investigate the discussion points from section 7.3:

- For each frequency, and over the output power range, find the optimum bias points and investigate the spread of these to understand the performance implications. This will include individual amplifier adjustments to address any balance issues.
- Investigate recovery time with the use of dual DACs, understand the potential for increased system linearity and efficiency.
- Holistic investigation of where the trade-off between the additional consumption of dual RF DACs and the discarded input power in the single input case can be found. To locate the point where the dual DAC approach achieves a higher overall system efficiency.

9. Summary

The opportunity to break the traditional performance limit of passive matching networks in RFPA design using load modulation techniques has been shared. An introductory explanation into the Load Modulated Balanced Amplifier, and its subtopic the Pseudo Doherty Load Modulated Balanced Amplifier, have been presented alongside practical measurement examples to assist theoretical validation on bespoke prototype hardware. Future challenge areas have been described to indicate the possible direction of future research.

10. References

1. "Broadband RF and Microwave Amplifiers", Andrei Grebenikov, Narendra Jumar, Binboga S. Yarman, 2017
2. "Chapter 8.2 The Doherty Amplifier, RF Power Amplifiers for Wireless Communications", Steve C. Cripps, 1999
3. "Electronically Reconfigurable Wideband High-Power Amplifier Architecture for Modern RF Systems (LMBA)", Daniel John Sheppard, 2018
4. "Dual-Octave-Bandwidth RF-Input Pseudo-Doherty Load Modulated Balanced Amplifier with ≥ 10-dB Power Back-off Range", Yuchen Cao and Kenle Chen, 2020